Bull. Korean Fish. Soc. 26(6), 538~548, 1993 韓水誌, 26(6), 538~548, 1993

The Effect of Wind Stress in the Southwestern Coastal Waters of the Japan Sea

Sun-Duck CHANG and Jong-Kyu KIM
Department of Ocean Engineering, National Fisheries University of Pusan, Pusan 608-737, Korea

In order to estimate the influence of wind stress in the southwestern coastal waters of the Japan Sea, the wind stress was estimated from the shipboard wind data of the Fisheries Research and Development Agency along the serial observation lines and Buoy No. 6 of the Japan Meteorological Agency. 5,100 wind data are used to construct a data set of monthly mean wind stress during 10 years from 1978 to 1987. The negative values of the mean zonal wind stress curl at Ulleung Basin in the study area seem to be responsible for the formation of the warm core. The volume transport of the East Korea Warm Current are estimated quantitatively by the variations of the Ekman transport associated with the reversing direction of the monsoon. And the distribution of the warm core is explained by the simple three layer model.

Introduction

The Japan Sea is a marginal sea surrounded by the Japanese Islands and the Asian continent. The major feature of the current system in the Japan Sea is an inflow of the Tsushima Current through the Korea Strait and the outflow through the Tsugaru and Soya Straits. The Tsushima Current has been known to split into three branches (Suda and Hidaka, 1932) in the southern region of the Japan Sea. The first branch is the bottom-controlled steady current subject to the topographic β-effect, the second branch is generated by the significant increase in inflow of the Tsushima Current in summer and the third one is a kind of the western boundary current due to the planetary β-effect (Kawabe, 1982a, b; Yoon, 1982a, b, c).

According to the monthly average of the depths of permanent thermocline and mixed layer in the Japan Sea, a pronounced spatial variation of the depth is present in north-south direction regardless of the season (National Federation of Fisheries Cooperatives, 1977). The region of the warm core coincides roughly with the latitude where the East Korea Warm Current separates from the Tsushima Current in the eastern coastal waters of Korea. It was also deduced from the trajectories of the drift bottles (Mitta and Kawatate, 1987). Na (1988b) tried to relate this semipermanent warm core with the wind distribution. The mechanism of the formation and sustain of the warm core is not yet clarified satisfactorily.

Historical wind data (Japan Meteorological Agency, 1972; Kutsuwada, 1982; Kutsuwada and Sakurai, 1982; Kutsuwada and Teramoto, 1987) depict a clear seasonal variation in wind stress over the Japan Sea and the northern Pacific. Moreover, a seasonal variation in wind stress might have a significant influence on the branching of the Tsushima Current and the current system of the Japan Sea (Sekine, 1986). Since the temporal change of the wind stress over the Japan Sea is large, a large variation in wind driven circulation is seen in his numerical experiment. The wind stress over the Japan Sea may be significantly influenced by the local effects such as the mountains stretching in north-south direction. Na (1988b) suggested that wind field in the Japan Sea is favorable to some extent

for the "saddle-like" feature of the warm core.

The main purpose of this study is to examine the effects of wind on the circulation and the warm core in the Japan Sea. The Ekman transport will be included for the estimation of the volume transport of the Tsushima Current through the Korea Strait.

Data and Methods

1. Data

Wind data were obtained from the reports by the FRDA (Fisheries Research and Development Agency) and the Japan Meteorological Agency. FRDA reports have the wind information measured by the Beaufort scale in 16 directions at the routine serial lines (Fig. 1). This routine survey has been made bimonthly.

Japanese data are from the Buoy No. 6 (Fig. 1) which measured the wind speed and direction every three hours. Wind data from the meteorological stations along the east coast of Korea may not be suitable for the calculation of sea surface wind stress due to local orographic conditions (Na, 1988a). From the wind data we have selected the winds that satisfy the dominance of the wind direction which is greater than 20% in frequency. Otherwise, wind data with the speed greater than 5*m/s* were selected. The distribution of winds from the serial observation lines (FRDA, 1978~1987) and Buoy No. 6 (JMA, 1977~1987) shown in Fig. 1 reveals that the northerly winds are dominant in winter whereas the southerly winds are dominant in summer. The zonally averaged maximum wind speeds at Line 106, Buoy No. 6 and Line 105 are presented in Table 1. While the wind at Buoy No. 6 was measured regardless of the weather the shipboard observation was not made during the stormy con-

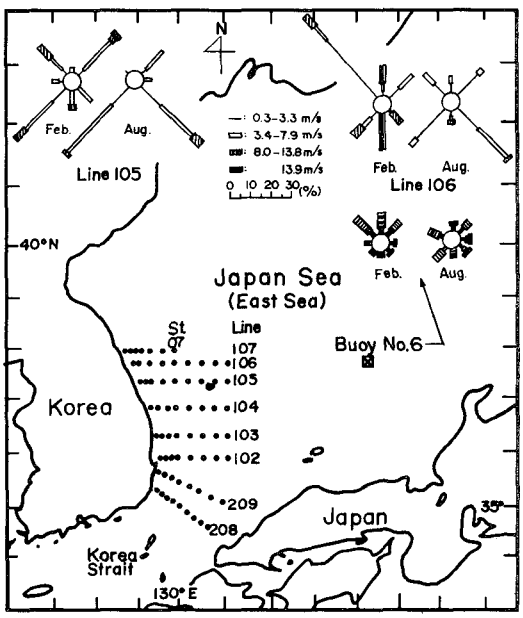

Fig. 1. Location and wind rose of the observation stations in the study area(FRDA, JMA; 1977~87)

Table 1. Composition of the zonally averaged maximum wind speeds in *m/s* at three locations

Month	Wind dir. (°)	Line 106 Freq. (%)	Line 106 Speed	Buoy No. 6 Freq. (%)	Buoy No. 6 Speed	Line 105 Freq. (%)	Line 105 Speed
Feb.	NE	15.0	5.0	9.9	29.2	7.9	5.0
	NW	53.3	10.0	15.5	30.1	25.0	7.5
	SE	6.7	12.5	3.4	16.5	13.2	12.5
	SW	11.7	10.0	2.7	27.5	40.8	12.5
Apr.	NE	18.9	8.7	16.3	24.1	11.1	7.5
	NW	8.4	8.7	20.1	28.2	14.4	7.5
	SE	33.7	11.1	14.0	24.5	44.4	12.5
	SW	23.2	9.9	19.2	27.7	20.0	12.5
June	NE	3.0	13.3	15.1	19.0	7.8	7.5
	NW	2.0	3.2	14.4	16.6	14.4	7.5
	SE	53.5	10.8	13.6	23.6	33.3	12.5
	SW	26.3	11.2	12.8	16.9	14.4	5.0
Aug.	NE	15.8	13.3	15.1	19.0	7.8	5.0
	NW	13.7	7.2	15.6	22.6	-	-
	SE	33.7	9.6	12.1	14.0	48.9	7.5
	SW	22.1	7.2	14.8	17.3	22.2	5.0
Oct.	NE	18.2	10.1	10.1	29.4	20.9	12.5
	NW	17.2	6.5	6.5	31.0	15.4	15.0
	SE	20.2	5.4	5.4	19.0	26.4	10.0
	SW	33.3	3.6	3.6	22.7	29.7	7.5
Dec.	NE	4.1	10.0	10.0	29.1	5.6	5.0
	NW	37.8	13.4	13.4	43.2	38.0	10.0
	SE	5.4	1.0	0.1	13.3	8.5	7.5
	SW	29.7	6.5	6.8	24.5	18.3	12.5

dition. As a result, the averaged maximum wind appeared much smaller at Line 106 and 105 than those observed at Buoy No. 6 (Table 1).

2. Computation of the wind stress

Annual mean and monthly mean wind stress fields over the Japan Sea are obtained using the data reports during ten years of 1978~1987. 5,100 data were used in the computation of wind stress. Thus, the zonal and meridional components of the wind stress are calculated from data reports.

We calculated the wind stress from the individual ship reports as measured at about ten meters height using the following bulk formula:

$$\tau_x=\rho_a C_D W W_x,\ \tau_y=\rho_a C_D W W_y \quad (1)$$

where τ_x and τ_y are the zonal (eastward) and meridional (northward) components of the wind stress, respectively, ρ_a is the air density, C_D is the drag coefficient, W is the wind speed, and W_x and W_y are the zonal and meridional components of the wind speed, respectively.

The drag coefficient C_D is considered dependent upon wind speed, sea state, and stability of the air. In earlier studies (Hidaka, 1958; Hellerman, 1967; Pond and Pickard, 1983; Kutsuwada, 1982; Kutsuwada and Sakurai, 1982), neutral stability was assumed and the drag coefficient was taken to be a function of the wind speed only. On the other hand, Hellerman and Rosenstein (1983) considered the effect of stability, and used a drag coefficient which is a function of both wind speed and the temperature difference between the air and the sea surface (Bunker, 1976).

Garratt (1977) summarized numerous previous studies on the determination of drag coefficient considering the linearly increasing relation with wind speed using the following regression formula:

$$C_D=(0.75+0.067\times|W|)\times10^{-3} \quad (2)$$

where W is the wind speed in *m/sec*.

Bunker (1976) used a drag coefficient which is a function of both wind speed and the temperature difference using the following formula:

$$C_D\times10^3=A_1+A_2W+A_3T-A_4W^2-A_5T^2-A_6WT \quad (3)$$

where, $A_1=0.934$, $A_2=0.0788$, $A_3=0.0868$, $A_4=0.000616$, $A_5=0.0012$, $A_6=0.00214$, W is the wind speed in *m/sec*, T (℃) is the difference of air temperature from SST (sea surface temperature). In this study, multiple regression formula (3) is employed for the computation of wind stress.

Fig. 2 and Fig. 3 show the wind speed, sea surface temperature, and air temperature from the Buoy No. 6 (JMA, 1977~87) and the serial observation lines (FRDA, 1978~1987), respectively. In this study, the air density ρ_a was taken to be a function of month and latitude and was calculated from averaged values of sea level pressure and air temperature data by Japan Meteorological Agency (1977) (Fig. 3). These values of monthly averages ranged from 1.210 to $1.256\times10^{-3} g\ cm^{-3}$ (Kutsuwada, 1982; Kutsuwada and Sakurai, 1982; Kutsuwada and Teramoto, 1987). The wind speed depends on the difference of the sea surface and air

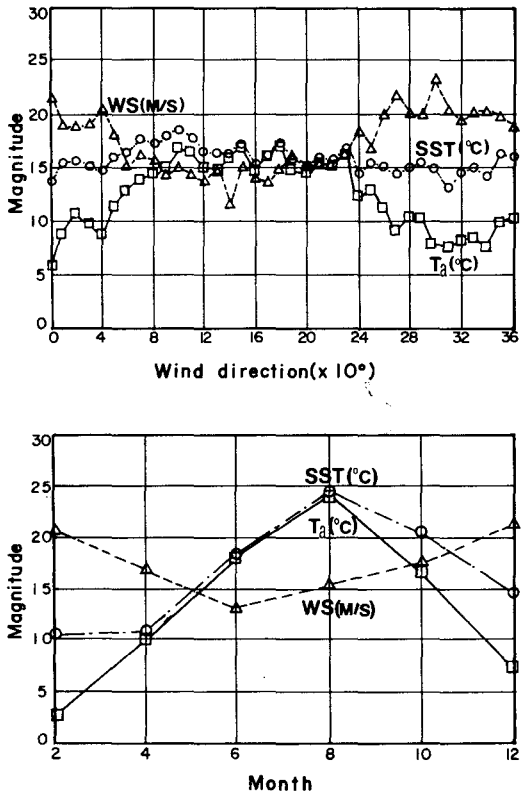

Fig. 2. Averaged wind speed(WS, daily maximum), sea surface temperature(SST), and air temperature(Ta)(Buoy No. 6, 1977~1987)

temperatures and is affected by the alternating monsoon. Fig. 4 shows the drag coefficients C_D in relation to the wind speed and SST-Ta in the bulk formula.

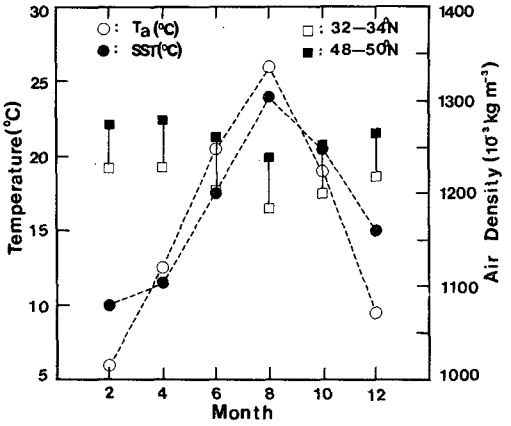

Fig. 3. Differences of the monthly averaged air density, air temperature(Ta) and sea surface temperature(SST)(JMA, FRDA; 1978~1987)

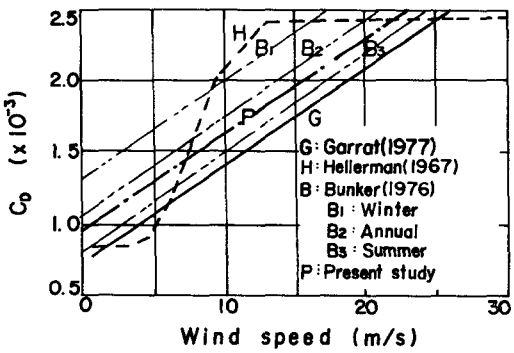

Fig. 4. The drag coefficients C_D in relation to the wind speed in the bulk formula

3. Wind stress curl, transports and the upper layer thickness

The distribution of wind stress has been used to explain the general features and transports of ocean circulation (Sverdrup, 1947; Munk, 1950). Such studies require the information on the distribution of wind stress curl.

The wind stress curl was computed using the following equation:

$$\mathrm{curl}_z \vec{\tau} = \frac{\partial \tau_y}{\partial x} - \frac{\partial \tau_x}{\partial y} \quad (4)$$

where τ_x and τ_y are the eastward and northward components of the wind stress, respectively. In this study, the meridional wind stress has been neglected, because East Korea Warm Current is considered to be predominantly a meridional transport the Korean Coast.

According to the classical ocean circulation theory initiated by Sverdrup (1947), the oceanic volume transport V in the interior of the ocean is related to the wind stress curl. In this study, the oceanic volume transport is obtained from the Ekman transport. Thus, the zonal and meridional components of the Ekman flux are given by

$$U_E = \frac{\tau_y}{\rho f}, \quad V_E = \frac{\tau_x}{\rho f} \quad (5)$$

where f is the Coriolis parameter and ρ is density of seawater.

We average the wind stress vectors in the two regions off the east coast of Korea and the western channel of the Korea Strait. Zonal transport U_E was neglected and V_E is calculated in the two regions by the Eq. (5) using the values of f at each serial observation lines and which is averaged over each area. Thus, volume fluxes and volume transports were estimated by the Ekman transport through the zonal boundaries in the study area.

In fact, the total transports in the upper layer consists of the Ekman transport and the geostrophic transport. The Ekman transport is usually ignored. It may not be proper to estimate the wind-driven transports over a relatively small area compared to the whole Japan Sea, and also the transport from other region and its effects on the mass distribution can not be ruled out.

But the computed magnitude of the wind stress curl which is very larger than the averaged value of the whole Japan Sea of Sekine (1986) should be explained to determine its role in transports and thus its relation to the thickness of the upper layer.

If there exists strong wind stress curl acting on the surface, the transport will be set up in relatively short period of time compared to the area under the weaker wind forcing. Thus, due to the spatial difference in magnitude of the wind stress curl

the change in thickness of the wind-influenced upper layer could occur within the small area compared to the whole Japan Sea.

By assuming three-layer ocean with the permanent thermocline and mixed layer as depth of interfaces, the thickness of the upper layer that is assumed change only by wind-driven transport of the upper layer can be obtained. For the three-layer system (Veronis, 1988), the heights $z=0$, $z=H_3$, $z=H_2$ and $z=H_1$ correspond, from the bottom to the bottom, the middle and the top layer, respectively (Fig. 5). In the present simplified calculation, the density stratification is idealized in terms of three homogeneous layers with uniform densities ρ_1, ρ_2, ρ_3 in the top, middle and bottom layer, respectively. The locations of the bounding surfaces are shown in Fig. 5 along with the thickness of each layer. In this model, the bottom layer is assumed motionless.

From the vertically integrated conservation equations for momentum and mass for the top and middle layers, the Sverdrup transport relation for the total mass transport, $\rho V \equiv \rho_1 V_1 + \rho_2 V_2$ follows,

$$\beta \rho V = \rho_1 \kappa \cdot \nabla \times \tau \qquad (6)$$

where $\beta = \frac{\partial f}{\partial y}$, $\kappa \cdot \nabla \times \tau = \frac{\partial \tau_x}{\partial y}$, κ is the vertical component of the wind stress curl.

The thickness of the upper layer, h, is given by the following equation,

$$\frac{1}{2}\frac{\partial}{\partial x}(g_1 h_1^2 + g_2 h^2) = [-f/\beta\, \partial \tau_x/\partial_y + \tau_x] \qquad (7)$$

where, x is positive eastward, h_1 and h_2 are the thickness of the top and middle layers, respectively, the right term is proportional to the vertical velocity induced at the base of the Ekman layer, and is independent of x, $g_1 = g\Delta\rho/\rho_3$, $g_2 = g(\rho_3 - \rho_2)/\rho_3$, $\Delta\rho$ is $(\rho_2 - \rho_1)$, g is gravity, $f = 2\omega \sin\phi$ is the Coriolis parameter, τ_x is the zonal component of the wind stress, ω is the angular frequency of the earth's rotation and ϕ is the latitude. Integration with respect to x yields

$$g_1 h_1^2 + g_2 h^2 = g_1 h_{1\times 0}^2 + g_2 h_{\times 0}^2 - 2[-f/\beta\, \partial \tau_x/\partial_y + \tau_x](x_0 - x) \qquad (8)$$

where $(\ )x_0$ is the value of $(\ )$ at $x = x_0$. At x_0 the zonal flow vanishes so the layer thicknesses must be constant.

The zonal transport equation with negligible meridional component of the wind stress is

$$f\, U = \frac{\partial}{\partial y}(g_1 h_1^2 + g_2 h^2) \qquad (9)$$

and it implies that with no zonal transport across the coast the thickness h is independent of y direction, i.e., in the north-south direction.

Eqation (8) gives some interesting information. The magnitude of the terms in the $[-f/\beta\, \partial\tau_x/\partial y + \tau_x]$, which depends on the latitude, will produce a latitudinal variation of h, the thickness of upper layer. Once the value of $\partial\tau_x/\partial y$ is known at some latitude, the east-west variations of h can be determined. Thus, for the present simplified three layer model, the sign and the magnitude of $\partial\tau_x/\partial y$ are the important factors in determining the local thickness of the upper layer. Since this model is for the large scale ocean circulation, more data covering the extensive area is desirable. However, unfortunately, the only available data are from the FRDA and Buoy No. 6.

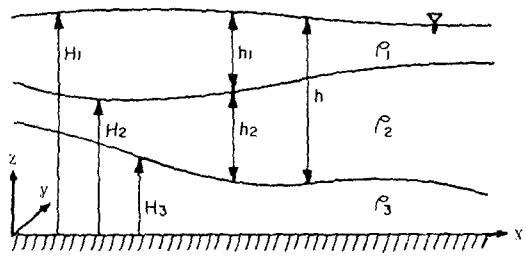

Fig. 5. Schematic representation of the three-layer model

Results and Discussion

1. Distribution of the wind stress

Fig. 6(c) shows the north-south variations of the zonal wind stress computed from the FRDA data for 10 years (1978~1987). The values obtained from the observations are indicated by the symbols corresponding to the serial observation lines (FRDA) from the Line 106 (upper) to the Line 102 (lower), respectively. The solid curve is obtained from a polynomial curve whose coefficients are determined by minimizing the squared error from

the observed points (Fig. 6). The difference in the magnitude of wind stress is clearly seen for both north-south directions and seasonally, i.e., the stronger wind stress during the winter months. The difference between previous studies (Sekine, 1986; Na, 1988a) and present study is caused by variation of the air density with latitude (Fig. 3). Therefore, reliable wind observations are necessary over the Japan Sea to consider the air density, SST-T_a, and to reduce uncertainty for the estimation of the wind stress.

The wind stress distribution that has been used for the numerical investigations of the Tsushima Current (Yoon a, b, c, 1982; Sekine, 1986) was such that wind stress becomes stronger northward during the winter monsoon and weaker but opposite in direction during the spring-summer season by the monthly mean wind stress data, 1958~75 (JMA, 1972; Kutsuwada, 1982; Kutsuwada and Sakurai, 1982). Thus an anticyclonic and a cyclonic wind stress imposed on the sea surface during the winter and summer season, respectively. With such wind stress, a gradual thinning of the upper layer northward over the whole Japan Sea can easily be expected (Sekine, 1986).

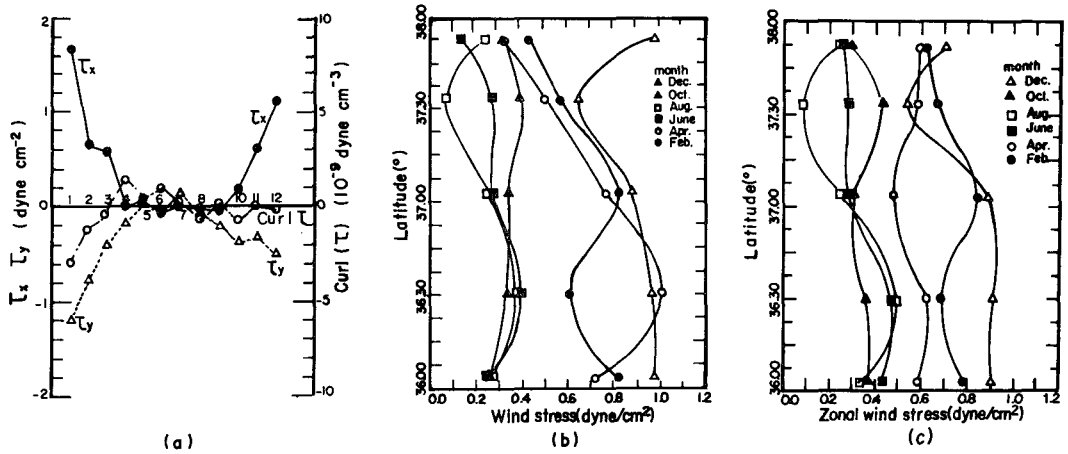

Fig. 6. Means of the monthly averaged wind stress: (a) Sekine(1986), (b) Na(1988a), (c) Present study

2. Variation of the wind stress curl and transports

Based on the Equation (6), Sverdrup transport and the pure Ekman transport due to wind stress for summer and winter have been calculated (Fig. 8(c)).

In Fig. 7(b), $\partial\tau_x/\partial y$ has been determined from the derivatives of the mean zonal wind stress shown in the Fig. 7(a). Fig. 8(c) shows the seasonal variations of the north-south transport in the eastern waters of Korea and the Korea Strait. Fig. 8(c) shows that the meridional Ekman fluxes in summer (June, Aug.) and winter (Dec., Feb.) are northward and southward probably in response to the south-eastward and north-eastward wind, respectively. Volume fluxes and volume transport was estimated by the Ekman transport through the zonal boundaries in the study area. Summations of the Ekman transports through the northern and the southern boundaries are about 0.61 Sv in summer and 1.4 Sv in winter. Fig. 8(c) shows that summations of the Ekman transports across the Line 209 and Line 208 boundaries are about 0.96 Sv in summer and 1.24 Sv in winter.

It is interesting to note that during the months of maximum northward transport through the strait the wind-driven northward flow is stronger than the flow of the winter season (Fig. 8(c)).

Furthermore, the wind-driven meridional transport is seasonally changing. The wintertime transport is twice stronger than that of summer and it could inhibit the northward flow of the Tsushima

Current through the Korea Strait to minimize the resultant volume transport during the winter season. Kang (1985) suggested that the heat content variation of the upper layer near the warm core seems to follow the annual fluctuation of the Tsushima Current in volume transport with time lag of a month.

Therefore it could be speculated that the Tsushima Current and its seasonal variation is influenced by the strength of southward flow driven by the wind stress over the Japan Sea. This is not a new idea, since under the distinct winter monsoon with their wind stress pattern the Ekman drift will be opposite to the northward flow through the strait (Huh, 1982) (Fig. 8). This study just shows the qualitative picture that explains the seasonal behavior of the meridional transport correponding to the Tsushima Current.

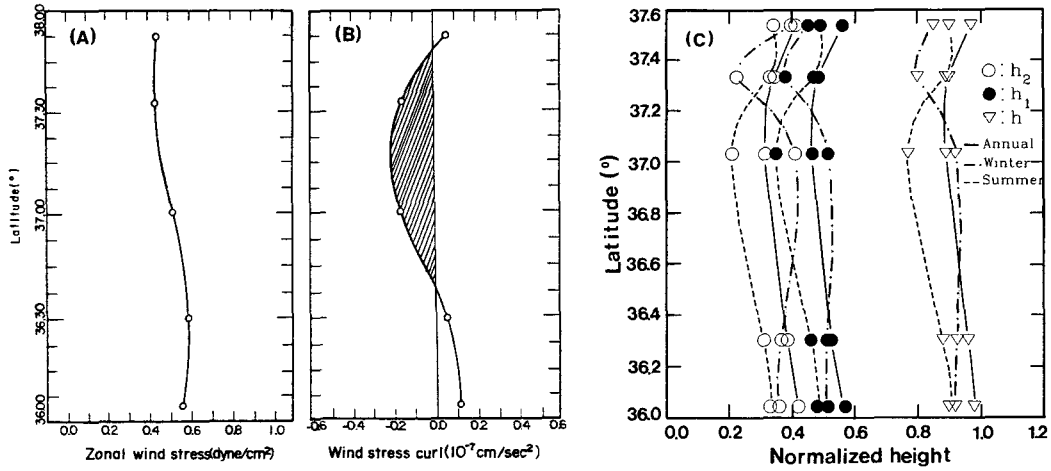

Fig. 7. Distribution of (a) the zonally averaged stress of zonal wind, (b) wind stress curl, (c) the height of interface(from the bottom)

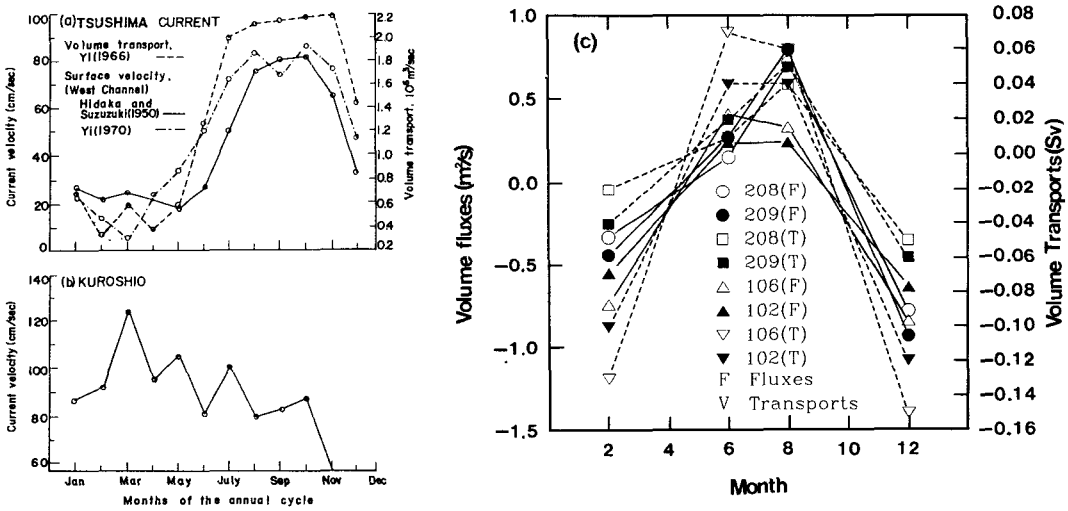

Fig. 8. The annual cycles of flow of the (a) Tsushima Warm Current, (b) mean monthly surface velocity of the Kuroshio, and (c) Volume fluxes in m^2/s and transports in Sv($=10^6 m^3/s$) estimated by the Ekman transport through zonal boundaries of the study area

3. Variation of the upper-layer thickness

For the present simplified three layer model, the sign and the magnitude of $\partial\tau_x/\partial y$ is important parameter in determining the local thickness of the upper layer. Further northern or southern extent of the τ_x distribution is desirable but not an essential factor for the present study. If the zonal variation of the wind stress over the Japan Sea exists, it may be necessary to see an east-west distribution of the upper-layer thickness in the study area.

Without considering the possible influx of the upper layer into the study area under consideration of the spatial distribution of the upper layer thickness or the height of the interfaces for the even months of the year shows that uneven distribution of the thickness with deeper layer being existed the warm core at Ulleung Basin (Fig. 9). The formation of thick upper layer or warm core is due to the transport of the upper layer water, and this can be easily verified by the distribution of the wind stress curl (Fig. 7).

From the Equation (6), the sign of $\partial\tau_x/\partial y$ determines the north-south flow so that convergence and divergence occur around 37°43'N and 36°30'N, respectively as the two-layer system (Na, 1988a). This means that, in the three-layer system, the thickness of the upper layer will be such that it becomes thick where the convergence occurs while it becomes thin where the divergence takes place.

The Fig. 7(c) shows the north-south distribution of a normalized height from the bottom interface that has been determined by use of the Equation (8).

The absolute magnitude of the thickness difference in the Fig. 7(c) can be estimated by selecting a value of the thickness at some longitude x_0, i.e., hx_0. To see the seasonal variations of the upper layer thickness, the months of June-August for summer and February-December for winter were chosen (Fig. 7(c)). Since the present simplified three-layer model could be applied to a seasonal or the permanent thermocline as the height of interfaces, the heights (Fig. 7(c)) can be compared with the one, corresponding to the months of August and December.

It should be noted that instead of the comparision between the values of the observed thickness and the those computed, it is rather important to find role of wind stress over the Japan Sea that acts positively in the formation of the warm core. Thus, the negative wind stress curl contributes to the formation of warm eddy (warm core) over the Japan Sea. At least, a qualitative comparison shows an agreement, in tendency of its north-south variations. It should also be noted that, since the wind fields have been zonally averaged, the same latitudinal variations of the depth must appear at any longitude. However, if any zonal variations of wind stress exist, the longitudinal variations of the depth should exist accordingly.

The Veronis' (1988) model only deals with the interior dynamics of the ocean with sharp east-west variations of the interface so that it can not be explained along the Korea coast. The Equation (8), however, describes the tendency of the shallow thermocline westward of the Japan Sea provided that the right terms are positive. But the tendency of the eastward shallow thermocline of the Japan

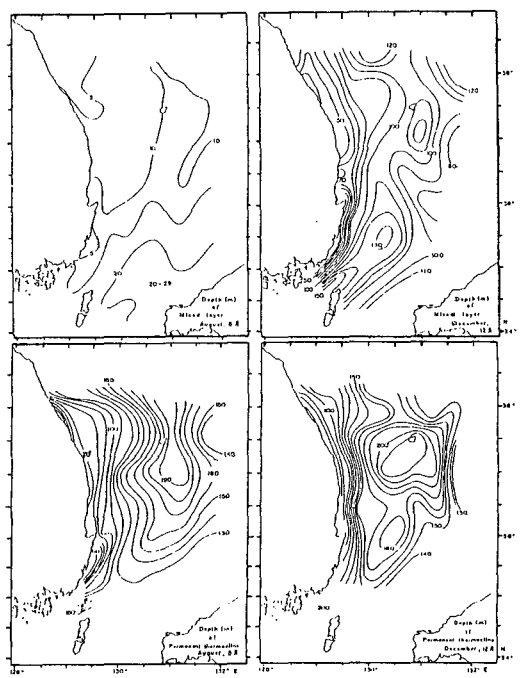

Fig. 9. Monthly averaged depth of the mixed layer and permanent thermocline in meters(National Federation of Fisheries Cooperatives, 1977)

Sea can not be explained. Therefore, reliable mechanism of the thermocline with consideration of the heat content is necessary to elucidate the circulation over the Japan Sea.

Summary and Conclusion

In order to estimate the influence of wind stress in the southwestern coastal waters of the Japan Sea, the wind stress was estimated from the shipboard wind data of the FRDA the serial observation lines and Buoy No. 6 of the Japan Meteorological Agency. 5,100 wind data are used to construct a data set of monthly mean wind stress during 10 years from 1978 to 1987. These monthly and annual mean wind stress distributions were put into the three-layer model which describes the latitudinal variations of the upper layer thickness and elucidates the seasonal variations of the transport by the Sverdrup relation and Ekman current.

The wind field contribute to maintain the almost time-independent distribution of the feature of the upper layer thickness in north-south direction and negative wind stress curl to maintain the formation of warm core over the Japan Sea. Elucidated is the variational characteristics of the East Korea Warm Current due to the variations of the zonally averaged wind stress (southward transport) from the seasonal variations of the meridional Ekman transport.

Because the shipboard observation is restricted to the relatively calm weather, more reliable Buoy data measured even in the severe conditions at several locations will be desirable for the estimation of wind stress and its curl.

References

Bunker, A. F. 1976. Computations of surface energy flux and annual air-sea interaction cycles of the North Atlantic Ocean. Mon. Wea. Rev. 104, 1122~1139.

Chang, S. D. 1970. Computation of wind drift currents in the southern waters of Korea. Bull. Korean Fish. Soc. 3(3), 199~206.

Chang, S. D. and J. K. Kim. 1991. Effect of wind stress on the sea water circulation in the south-western Japan Sea. JECSS, 6th, 77.

Garratt, J. 1977. Review of drag coefficients over oceans and continents. Mon. Wea. Rev. 109, 1190~1207.

Hantel, M. 1972. Wind stress curl - the forcing function for oceanic motions. Physical Oceanography, 121~136.

Hellerman, S. 1967. An updated estimate of the wind stress on the world ocean. Mon. Wea. Rev. 95, 607~614.

Hellerman, S. and M. Rosenstein. 1983. Normal monthly wind stress over the world ocean with error estimates. J. Phys. Oceanogr. 13, 1093~1104.

Hidaka, K. 1958. Computation of the wind stresses over the ocean. Records of Oceanographic Works in Japan, 4, 77~123.

Huh, O. K. 1982. Spring season stagnation of the Tsushima Current and its separation from the Kuroshio:Satellite evidence. J. of Geophy. Res. 87. C12, 9687~9693.

Japan Meteorological Agency, Marine Department. 1977. Marine climatological tables of the North Pacific Ocean for 1961~1970, 180.

Kang, Y. Q. 1985. Seasonal variation of heat content in the neighbouring seas of Korea. J. of Oceanol. Soc. Korea, 20(3), 1~5.

Kawabe, M. 1982a, b. Branching of the Tsushima current in the Japan Sea, Part I, II. J. of Oceanol. Soc. Japan, 38, 95~107, 183~192.

Kutsuwada, K. 1982. New computation of wind stress over the North Pacific Ocean. J. of Oceanol. Soc. Japan, 38, 159~171.

Kutsuwada, K. and K. Sakurai. 1982. Climatological maps of wind stress field over the North Pacific Ocean. Oceanogr. Mag. 32(1~2), 25~46.

Kutsuwada, K. and T. Teramoto. 1987. Monthly maps of surface wind stress fields over the North Pacific during 1961~1984. Bull. of Ocean Res. Inst. Univ. Tokyo, No. 24, 1~100.

Mitta, T. and K. Kawatate. 1987. Trajectories of drift bottles released in the Tsushima Strait. Progr. in Oceanogr., PERGAMON Press, 17,

255~264.

Munk, W. H. 1950. On the wind-driven ocean circulation. J. of Meteo. 7, 79~93.

Na, J. Y. 1988a. Spatio-temporal distributions of the wind stress and the thermocline in the East Sea of Korea. Bull. Korean Fish. Soc. 21(6), 307~316.

Na, J. Y. 1988b. Wind stress distribution and its application to the upper layer structures in the East Sea of Korea. J. of Oceanol. Soc. Korea, 23(3), 97~109.

National Federation of Fisheries Cooperatives. 1977. Oceanographic environments and fisheries resources of the east coast of Korea. National Federation of Fisheries Co., Korea, p. 435.

Pond, S. and G. L. Pickard. 1983. Introductory Dynamical Oceanography. PERGAMON Press, p. 329.

Sekine, Y. 1986. Wind-driven circulation in the Japan Sea and its influence on the branching of the Tsushima current. Progress in Oceanography, PERGAMON Press, 7, 297~312.

Suda, K. and K. Hidaka. 1932. The results of the oceanographical observation on board R. M. S. 'Syunpu Maru' in the southern part of the Japan Sea in the summer of 1929, part I. J. Oceanogr. Imp. Mar. Observ. 3, 291~375.

Sverdrup, H. U. 1947. Wind-driven current in a baroclinic ocean; with application to the equatorial currents of the eastern Pacific. Proc. Nat. Acdd. Sci. 33(11), 318~326.

Veronis, G. 1988. Circulation driven by winds and surface cooling. J. of Phys. Oceanogr. 18, 1920~1932.

Yoon, J. H. 1982a, b, c. Numerical experiment on the circulation in the Japan Sea, part I, II, III. J. Oceanol. Soc. Japan, 38, 43~51, 81~94, 125~130.

Received July 1, 1993
Accepted November 6, 1993

東海 沿岸域 海水循環에 대한 바람응력 效果

張善德 · 金鍾圭
釜山水產大學校 海洋工學科

韓國 東海 沿岸域 海水循環 및 水溫分布에 대한 바람응력의 效果에 관하여 檢討하였다. 東海上의 바람응력은 國立水產振興院 停船觀測 바람자료 및 日本氣象廳 Buoy No. 6에서의 10년간(1978~1987)의 약 5,100개의 바람 觀測資料를 사용하여 계산하였다. 여름과 겨울의 季節風의 轉換에 따른 에크만 輸送의 變化가 大韓海峽에서의 대마난류 輸送量에 미치는 影響을 定量的으로 評價하였다. 특히 東海에서의 平均的인 바람응력의 回轉性(wind stress curl) 값이 陰이 되는 사실에서 鬱陵島 近海의 暖水層의 形成에 部分的으로 도움이 됨을 알았다. 한편, 東海 暖水層의 分布를 單純化된 3層 境界面모델을 適用하여 說明하였다.